

Solar Wind Helium Ions: Observations of the Helios Solar Probes Between 0.3 and 1 AU

E. MARSCH,¹ K.-H. MÜHLHÄUSER,² H. ROSENBAUER,¹
R. SCHWENN,¹ AND F. M. NEUBAUER³

A survey of solar wind helium ion velocity distributions and derived parameters as measured by the Helios solar probes between 0.3 and 1 AU is presented. Nonthermal features like heat fluxes or He^{2+} double streams and temperature anisotropies have been frequently observed. Fairly isotropic distributions have only been measured close to sector boundaries of the interplanetary magnetic field. At times in slow solar wind, persistent double-humped helium ion distributions constituting a temperature anisotropy $T_{\parallel\alpha}/T_{\perp\alpha} > 1$ have been reliably identified. Distributions in high-speed wind generally have small total anisotropies ($T_{\parallel\alpha}/T_{\perp\alpha} \approx 1$) with a slight indication that in the core part the temperatures are larger parallel than perpendicular to the magnetic field, in contrast to simultaneous proton observations. The anisotropy tends to increase with increasing heliocentric radial distance. The average dependence of helium ion temperatures on radial distance from the sun is described by a power law $\sim R^{-\beta}$ with $0.7 \leq \beta \leq 1.2$ for $T_{\parallel\alpha}$ and $0.87 \leq \beta \leq 1.4$ for $T_{\perp\alpha}$. In fast solar wind the $T_{\perp\alpha}$ profile is compatible with nearly adiabatic cooling. Pronounced differential ion speeds Δv_{ap} have been observed with values of more than 150 km/s near perihelion (0.3 AU). In fast streams Δv_{ap} tends to approach the local Alfvén velocity v_A , whereas in slow plasma values around zero are obtained. Generally, the differential speed increases with increasing proton bulk speed and (with the exception of slow plasma) with increasing heliocentric radial distance. The role of Coulomb collisions in limiting Δv_{ap} and the ion temperature ratio T_{α}/T_p is investigated. Collisions are shown to play a negligible role in fast solar wind, possibly a minor role in intermediate speed solar wind and a distinct role in low-speed wind in limiting the differential ion velocity and temperature.

1. INTRODUCTION

This paper presents a survey of Helios observations of helium ion three-dimensional velocity distributions in the solar wind and of parameters derived from them. The close approaches to the sun of both Helios 1 (0.30 AU in perihelion) and Helios 2 (0.29 AU in perihelion) provided the opportunity to make the first in situ measurements of interplanetary plasma inside the orbit of Mercury and to study radial variations of solar wind parameters and ion distributions between 0.3 and 1.0 AU. The following results are based on the data set of the primary missions of the Helios probes (from date of launch to about 110 days later). The spacecraft, payload, and experiment have been described earlier [Schwenn *et al.*, 1975; Rosenbauer *et al.*, 1977]. A detailed description of the plasma data evaluation procedure is given in a companion paper concerned with simultaneous proton observations [Marsch *et al.*, this issue]. The magnetometer data used in this study have been obtained by the TU Braunschweig magnetometer experiment [Musmann *et al.*, 1975; Neubauer *et al.*, 1977].

Long-time averages of bulk speed ratios of helium and hydrogen have yielded values for v_{α}/v_p of about 1 with a slight skewing of the frequency distribution to values greater than 1 [Robbins *et al.*, 1970; Formisano *et al.*, 1970; Asbridge *et al.*, 1976]. The occurrence of pronounced speed differences has been reported with experimental confidence

by many authors [Formisano, *et al.*, 1970; Asbridge *et al.*, 1974; Hirshberg *et al.*, 1974; Ogilvie, 1975; Bosqued *et al.*, 1976; Grünwaldt and Rosenbauer 1978]. The value of determining long-time averages of the bulk speed ratio can be questioned because, in our opinion, insight into the physical processes is gained only by much more detailed studies such as have been initiated by Asbridge *et al.* [1976], Grünwaldt and Rosenbauer [1978], and Neugebauer [1981]. These works lead to the conclusion that wave-particle interactions might account for the observed preferential acceleration of He^{2+} up to the local Alfvén speed in high-speed streams [Marsch *et al.*, 1981a]. It was also emphasized in these works that the influence of Coulomb collisions deserves further careful investigation. In this paper a thorough study is presented of bulk speed differences between the two most abundant solar wind ions, helium and hydrogen. The correlation of the bulk velocity difference $\Delta v_{ap} = v_{\alpha} - v_p$ with the solar wind velocity and the radial evolution of Δv_{ap} (within the orbital range of the Helios probes) is examined. Also, the role of Coulomb collisions in limiting ion differential flow will be investigated.

The observation of velocity differences between the two major ion components in the solar wind initiated a lot of theoretical work. The older theories, as reviewed in the work of Hundhausen [1972] could not explain the equalization of hydrogen and helium ion speeds when the two components exchange momentum and energy only via Coulomb collisions. Even models invoking preferential acceleration of minor ions by Alfvén wave pressure forces [Hollweg, 1974] could barely explain the equal bulk speeds under slow wind conditions, much less the fact that in fast wind the helium velocity persistently exceeds the hydrogen velocity. Other models assumed high coronal temperatures for heavy ions [Ryan and Axford, 1975] to fit the observations. A first step toward a refined theory including resonant wave-particle interactions leading to preferential acceleration has re-

¹ Max-Planck-Institut für Aeronomie, D-3411 Katlenburg-Lindau 3, Federal Republic of Germany.

² Max-Planck-Institut für Physik und Astrophysik, Institut für extraterrestrische Physik, D-8046 Garching, Federal Republic of Germany.

³ Institut für Geophysik und Meteorologie der Technischen Universität Braunschweig, D-3300 Braunschweig, Federal Republic of Germany.

cently been made by *Hollweg and Turner* [1978], *McKenzie et al.* [1978, 1979], *Hollweg* [1981], *Dusenbery and Hollweg* [1981], and *McKenzie and Marsch* [1981]. With the present paper, we introduce into this discussion new observational findings.

The weakly collisional nature of the solar wind manifests itself naturally not only in unequal bulk speeds but also in unequal temperatures and temperature anisotropies of both ion species. This observation has also provoked a lot of theoretical work by many authors. A reference list can be found in the papers by *Feldman et al.* [1974a] and *Neugebauer* [1976], which concentrate exclusively on the solar wind ion temperature ratio T_{α}/T_p . These authors have done a careful study of the regulation of T_{α}/T_p by the ratio of solar wind expansion and collisional energy exchange time τ_{exp}/τ_{ap} and have empirically derived a statistical relationship between these parameters. Our paper gives an extension of their analysis to heliocentric distances between 1 and 0.3 AU. It may be emphasized, however, that because of the three-dimensional measurement of the Helium ion distribution, detailed information about the total temperature tensor is available. Thus the He^{2+} temperature anisotropy itself is investigated as well.

Among the nonthermal features of solar wind helium distributions observed at 1 AU are double-peaked spectra [*Feldman et al.*, 1974b]. Persistent spectra of this type have also been obtained by the Helios plasma analyzers, especially in low-speed plasma, temporarily giving rise to large temperature anisotropies $T_{\parallel\alpha}/T_{\perp\alpha} > 1$ and pronounced heat fluxes [*Marsch et al.*, 1981a]. In this paper we present a study of second and third moments of helium three-dimensional velocity distributions.

The observational determination of at least average heliocentric radial gradients of plasma parameters is of extraordinary importance for a comparison with any solar wind theory, because such measured gradients provide further constraints that must be satisfied in addition to the boundary conditions commonly derived from 1 AU observations. A very fruitful attempt has been made to analyze plasma at different radial solar distances by *Schwenn et al.* [1981]. Owing to the favorable Helios orbits, radial gradients of solar wind parameters could be derived from radial line-up configurations of the two probes. By in situ measurement, basic differences in the microstate of the fast and slow solar wind during the expansion within identical flux tubes were confirmed to exist. Though promising, these studies are limited by the finite data sets fulfilling the requirements of a strict line-up. Therefore this paper presents radial dependences for helium ion parameters obtained by averaging the plasma parameters, but only after separation of the data into classes of different solar wind velocities to avoid mixing noncomparable states of the wind.

2. PHENOMENOLOGICAL SURVEY OF THE MOMENTS OF HELIUM ION VELOCITY DISTRIBUTIONS

An overview of the main helium ion parameters as observed during three successive solar rotations of the Helios 2 primary mission, i.e., during the first 80 days after launch in January 1976, is given in Figure 1. One hour averages of bulk speed v_{α} , density n_{α} , temperature parallel ($T_{\parallel\alpha}$), and (indicated by dots) perpendicular ($T_{\perp\alpha}$) to the magnetic field direction, and the absolute value of the heat flux density vector of

helium ions are plotted versus Carrington longitude. For reference the proton bulk speed has been marked by points in the first panel. The heliographic latitude of the spacecraft position and its distance from the sun in AU are given at the bottom of each panel. Also the days of the year 1976 are indicated along the abscissa. The radial interval of the three plots extends from 0.983 to 0.409 AU. Data gaps for rotation 1638 are due to the fact that in the perihelion region, especially in low-speed plasma, the electrodynamic mass spectrometer, which measures only pure proton distributions, was operating. Therefore no three-dimensional He^{2+} distributions are available for these time periods. For all other time intervals showing data gaps a reliable helium ion data evaluation was not possible.

Two corotating high-speed streams can be recognized in Figure 1. A general tendency of the fast stream plasma to be hotter than the slow stream plasma is clearly visible from the first and third panel. This confirms observations in the earth's orbit [*Neugebauer and Snyder*, 1966; *Hirshberg et al.*, 1974; *Feldman et al.*, 1974a]. The variation of the helium temperature appears very similar to that of the bulk velocity. (These observations correspond to those for hydrogen velocity and temperature that have been presented for the primary mission of Helios 1 by *Rosenbauer et al.* [1977] and for Helios 2 by *Marsch et al.* [this issue].) An empirical temperature-speed correlation of the type found for protons by *Burlaga and Ogilvie* [1973] may thus also be established for helium ions in the solar wind. Inspection of the last panels of each solar rotation shows that the variations in the heat flux and in the temperature are intimately correlated. The helium ion heat flux varies between 10^{-6} and 10^{-3} erg cm^{-2} s^{-1} , which is almost three orders of magnitude less than the electron heat flux in comparable solar wind states. The discussion by *Marsch et al.* [this issue] of the proton heat flux Q_p holds also for Q_{α} : The similar profiles of heat flux density Q_{α} and parallel temperature $T_{\parallel\alpha}$ suggest that Q_{α} is not related to a temperature gradient in the classical sense. Q_{α} may simply serve as an indicator of higher order asymmetries in the gyrotropic helium ion distributions along the local magnetic field. One should bear in mind, however, that Q_{α} is even more sensitive to errors in the data evaluation than Q_p , both because of the poor statistics in the counting rates and because of the uncertainties in the ion separation procedure.

Regarding the helium bulk velocity profiles in Figure 1 the same tendency as observed for protons may be noticed, namely that the leading edges of fast streams steepen closer to the sun. This observation is also supported by the Helios 1 data which are not shown here. Like the proton fast streams [*Schwenn et al.*, 1978], high-speed helium streams also show sharp latitudinal boundaries that are generally thinner at 0.3 AU than at 1 AU. At 0.3 AU the relative bulk speed increase across the stream front is even more pronounced for helium than for hydrogen ions because in slow speed plasma He^{2+} tends to lag behind the protons by a few kilometers per second, whereas in high-speed plasma He^{2+} moves as much as 150 km/s faster than the protons. As is discussed below, large variations in the ion temperature ratio and differential speed indicate that considerable differences occur on the microscopic level of the distribution functions of the two ion species. But no indications of basic differences on a macroscopic level (spatial extent, boundaries, and global geometry

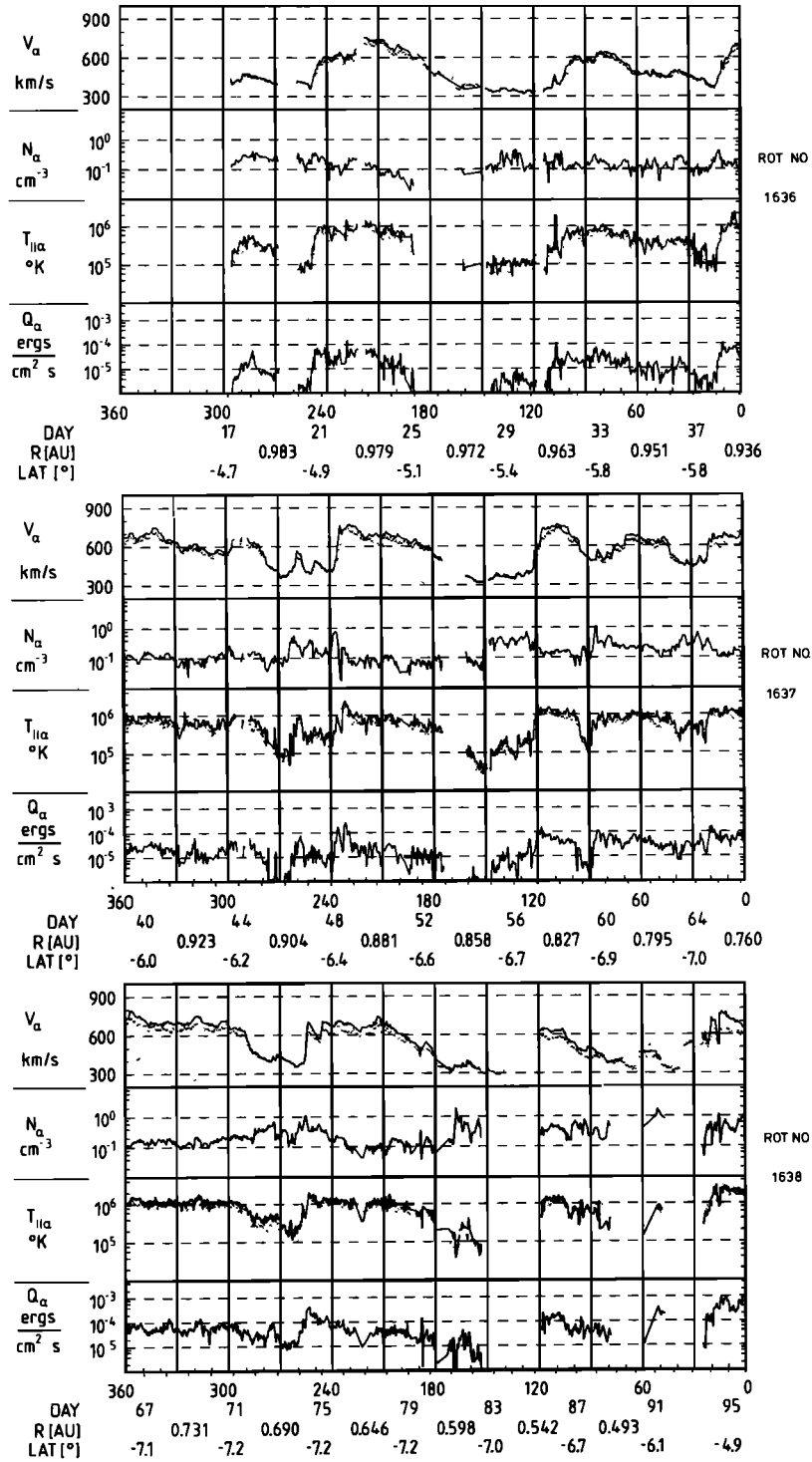


Fig. 1. One-hour averages of solar wind helium ion bulk speed (proton bulk speed indicated by points), number density, temperature $T_{II\alpha}$ ($T_{\perp\alpha}$ indicated by points), and the heat flux density are shown versus Carrington longitude for three successive solar rotations. Time of measurement, radial heliocentric distance, and solar latitude are given along the abscissa. The data have been obtained by Helios 2 between January 17, 1976, and April 5, 1976, when the satellite traversed a radial distance from 0.98 to 0.41 AU.

of the stream structure) have been found so far within the Helios orbits.

Note another observation in Figure 1 (compare for example data at about day 21, 31, 38, 48, 74, 94) at the steep rise to a high-speed stream. Density enhancements and spikelike increases in the temperature and heat flux density often

appear in the middle of the leading edge of high-speed streams characterizing the compression region. A similar finding is well-known from proton measurements and has also been reported for helium in the near earth orbit region by *Hirshberg et al.* [1974]. Stream interfaces certainly deserve a detailed study of their own as was done by *Burlaga*

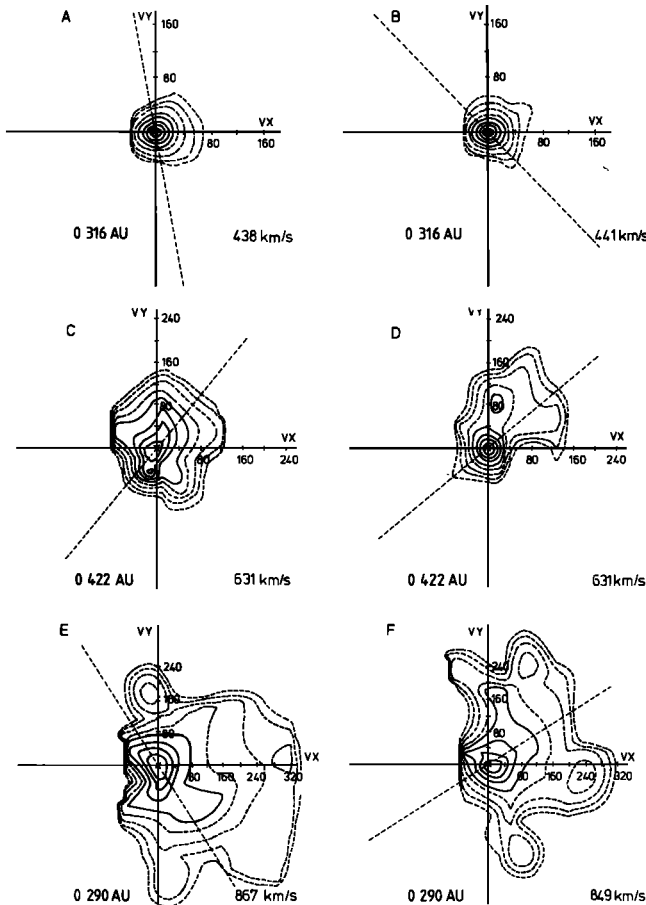


Fig. 2. Helios 2 helium ion three-dimensional velocity distributions as measured for various solar wind velocities (increasing from top to bottom). The cuts through the distributions are provided in a plane defined by the bulk velocity vector (VX axis) and the magnetic field vector (dashed line). Contour lines correspond to fractions 0.8, 0.6, 0.4, and 0.2 (continuous lines) and to logarithmically spaced fractions 0.1, 0.032, 0.01, and 0.0032 (dashed lines) of the maximum phase space density. The origin of velocity space has been chosen at the velocity of the maximum phase density and scales are given in km/s. Relevant plasma parameters are listed in Table 1.

[1974] and by Gosling *et al.* [1978]. This is, however, not the intent of the present paper. Finally, a rough impression about radial gradients in temperature and heat flux density may be obtained from Figure 1. If parameters in fast streams of equal bulk speed are compared, a slight increase in temperature with decreasing radial distance can be inferred. The gradients in the heat flux density seem to be more pronounced, which is understandable because of the proportionality of Q_{α} to the number density.

3. OBSERVED FEATURES OF HELIUM ION VELOCITY DISTRIBUTIONS

This section illustrates some features of helium ion velocity distributions observed between 0.3 and 1 AU. For further details regarding instrumentation and data evaluation, see Schwenn *et al.* [1975] and Rosenbauer *et al.* [1977]. The problems involved in interpreting the measured spectra in

terms of different ion species are discussed by Marsch *et al.* [this issue]. In the present context a few remarks are sufficient. The three-dimensional Helios plasma analyzer measures energy per charge (E/q) spectra in 32 channels exponentially spaced between 155 V and 15.3 kV. Angular resolution is achieved in azimuth by use of the spacecraft's rotation and in elevation by individual particle detectors (channeltrons at 5° intervals). Two main peaks that usually occur in the spectra are commonly attributed to hydrogen and helium ions. Therefore a separation of the count rates pertaining to the two different kinds of ions is necessary. This is achieved by cutting the spectra at the relative minimum between the main peaks in an appropriate way. (See extensive discussion of this topic in Marsch *et al.* [this issue].) In most cases a clear identification of the helium ions was possible and a reliable separation of the species could be made.

The three-dimensional velocity space resolution of the Helios instrument makes the separation of helium ions and protons easier than with past measurements. Only if the magnetic field is radial or the ion temperatures are high, do high-energy extensions of the proton distributions mix with the He^{2+} distributions. Unfortunately, this does occur, particularly in hot fast stream distributions. Under those conditions some ambiguity is certainly introduced in the ion separation procedure.

A steep decline of the He^{2+} distributions on the low velocity side may partially be an artifact owing to erroneous assignment of counting rates to the two ion species in the measurement channels where the distributions overlap. (See, for example, the last panel of Figure 2, which is discussed below; the true distributions would possibly extend further along the negative VX axis). Since count rates for He^{2+} were not extrapolated into the overlapping region, we may occasionally have slightly underestimated the temperatures $T_{\parallel\alpha}$, $T_{\perp\alpha}$ and density n_{α} and overestimated the bulk velocity v_{α} and the heat flux density vector Q_{α} . However, by checking these effects for individual spectra it has been ascertained that the derived moments (with the exception of Q_{α}) are not influenced significantly by the separation method.

Another principal problem is caused by the time-varying and occasionally low He^{2+} content in the solar wind. If the helium ion flux is very low, the sensitivity of the plasma analyzer is marginal for resolving the detailed structure of the distribution. However, in many cases it is possible to evaluate three-dimensional helium ion distributions, whose shape and details are statistically significant in the core parts. In the following we concentrate on a few selected examples, where the statistical errors were small.

In Figure 2 cuts through helium ion three-dimensional distributions are shown in a plane defined by the bulk velocity direction (VX axis) and the magnetic field direction (indicated by the dashed line). The origin of velocity space has been chosen at the maximum phase space density. Numerical values are given in Table 1 (in the column indicated by f_{max}). Continuous contour lines correspond to fractions 0.8, 0.6, 0.4, and 0.2 of the maximum, and dashed lines correspond to logarithmically spaced fractions 0.1, 0.032, 0.01, and 0.0032, respectively. In the upper panel (cases A and B) are shown some fairly isotropic distributions

TABLE 1. Solar Wind Parameters for Figures 2 and 3

Day, 1976	Time, UT	R , AU	$ v_{\alpha} $, km/s	n_{α} , cm $^{-3}$	$T_{\parallel\alpha}$, 10 50 K	$T_{\perp\alpha}$, 10 50 K	B_z , 10 $^{-5}$ G	α_B , deg	ϵ_B , deg	$ \Delta v_{\alpha p} $, km/s	v_A , km/s	f_{MAX} , 10 $^{-20}$ cm $^{-6}$ s 3	Letter
102	1832:45	0.316	438	5.17	2.08	2.36	3.4	-85.9	-42.7	3.6	4.7	20.71	A
102	1840:51	0.316	441	5.67	2.19	1.86	12.1	-54.2	-1.1	1.5	16.4	27.88	B
94	0107:50	0.422	631	0.43	8.25	7.95	26.3	27.3	37.8	60.0	134.7	0.06	C
94	0110:32	0.422	631	0.27	10.25	7.19	26.7	21.1	29.7	76.4	137.5	0.07	D
108	0101:14	0.290	867	0.88	45.44	36.47	44.5	-179.1	-30.5	172.2	152.7	0.02	E
108	0105:57	0.290	849	1.14	45.04	32.73	41.8	118.5	-5.0	151.1	160.5	0.03	F
72	1000:35	0.697	453	0.40	3.66	1.72	9.6	-12.1	-29.6	8.2	59.8	1.30	A1
72	1001:56	0.697	443	0.42	4.43	1.78	9.6	-8.1	-26.2	3.7	58.6	0.57	B1
72	1010:02	0.696	447	0.38	4.53	1.41	9.6	-14.4	-27.2	10.4	60.3	0.41	C1
72	1018:48	0.696	432	0.37	3.56	2.84	9.6	-16.1	-25.3	17.6	63.0	0.32	D1

that have been measured in a low-speed region close to a magnetic sector boundary at 0.316 AU. In these particular cases the Helium ion number density was $n_{\alpha} \approx 5$, and the proton density was $n_p \approx 230$. The thermal speed amounted to about 21 km/s for both distributions. The bulk velocity vectors of the two ion species were practically equal during this time period ($|\Delta v_{\alpha p}| < 5$ km/s and $v_{\alpha} \approx 440$ km/s). Relevant plasma parameters are listed in Table 1. (For the complete ion spectra compare Figures 1 and 2 of the paper by Marsch *et al.* [this issue].)

The second panel in Figure 2 (cases C and D) displays distributions that have been measured in a high speed stream at 0.42 AU. One can recognize the higher temperature (note the extended velocity scale) and an indication that $T_{\parallel\alpha}$ is larger than $T_{\perp\alpha}$. It should be emphasized that details below the level corresponding to the last continuous contour lines are not very reliable and often accidentally produced by poor statistics. This applies to both the middle and the lower panel.

Feldman *et al.* [1973, 1974b] and Marsch *et al.* [this issue] have reported the occurrence of large temperature anisotropies in the core of proton high speed distributions, where as a rule $T_{\parallel c}/T_{\perp c} < 1$. In order to investigate whether this feature also exists in helium ion distributions, Gaussian least squares fits have been applied to the data points within the continuous contour line system above 10% of the maximum phase space density. In this way we have established that, in contrast to the proton distributions, $T_{\parallel c}/T_{\perp c} > 1$ is common in high-speed helium ion distributions. This finding is illustrated in the last panel of Figure 2 (cases E and F), which shows distributions as measured in a very fast stream at 0.29 AU. The reader should inspect Figure 16 of the companion paper by Marsch *et al.* [this issue] where similar observations are exhaustively discussed. These results suggest that the two ion species are affected differently by the processes that heat solar wind streams. Note from Table 1 the extremely high helium total temperature (more than four times that of the protons) and also that the helium ions (in the cases E and F) move more than 150 km/s faster than the protons. Ion differential speeds are fully investigated in section 5.

Frequently, magnetic-field-aligned bulges constituting a total temperature anisotropy $T_{\parallel\alpha}/T_{\perp\alpha} > 1$ and a heat flux are evident in the distributions, as can be seen in the middle and bottom panel of Figure 2. Sometimes even a clearly resolved second peak evolves as demonstrated in Figure 3. Similar observations have been reported earlier by Asbridge *et al.* [1974] from measurements at 1 AU. In the distributions

shown in Figure 3, the second He^{2+} hump moves relative to the main peak along the local magnetic field direction with a drift speed of about $v_D \approx 40\text{--}60$ km/s. Corresponding characteristic plasma parameters are also listed in Table 1. Owing to the three-dimensional resolution of the Helios plasma analyzer it was possible to identify these He^{2+} double streams, though the magnetic field was pointing out of the ecliptic plane with an elevation angle of $\epsilon_B \approx -26^\circ$. The exemplary distributions shown were observed at 0.697 AU under very stationary solar wind conditions. It should be mentioned that due to the oblique magnetic field no confusion of He^{2+} with heavier minor ions was possible. Namely, according to their larger ratio of mass to charge in comparison with He^{2+} these ions are expected to be found on the positive VX axis of Figure 3 in a region, which is located considerably away from the velocity origin. A thorough discussion of the problems involved in identifying heavy minor ions in E/q spectra can be found in the paper by Schwenn *et al.* [1980].

Figure 4 demonstrates the persistence of the double peak phenomenon. For a time interval of about six hours on day 72 in 1976 ion count rate spectra integrated over both angles of incidence are shown as functions of the energy per charge channel numbers of the instrument. Successive spectra have been plotted one below the other in order to clearly indicate possible changes in their shape. Time is running from above to below and given in hours and minutes. The main ridge corresponds to protons whereas the second hump starting at channel 16 pertains to helium ions. Both ridges are doubly peaked. Despite large fluctuations, a resolved and stationary two-peak structure is observed in the He^{2+} spectra. (The arrow marks the time where the distributions shown in Figure 3 were taken). Figure 4 provides convincing evidence that helium ion double peaked distributions occur in the solar wind and can be quite constant in shape during a relatively long time period. The corresponding three-dimensional proton distributions have been shown in Figure 6, letter B1, of the paper by Marsch *et al.* [this issue]. The ion species had nearly equal bulk velocities during this time period. The drift speed between the two components of the helium and hydrogen ion distributions, respectively, was on the average nearly equal to the local Alfvén speed v_A , which amounted to about 60 km/s for several hours. The whole structure looked like two ‘interpenetrating’ solar wind streams moving relative to each other with the Alfvén velocity. A similar observation at 1 AU has been reported before by Feldman *et al.* [1974b].

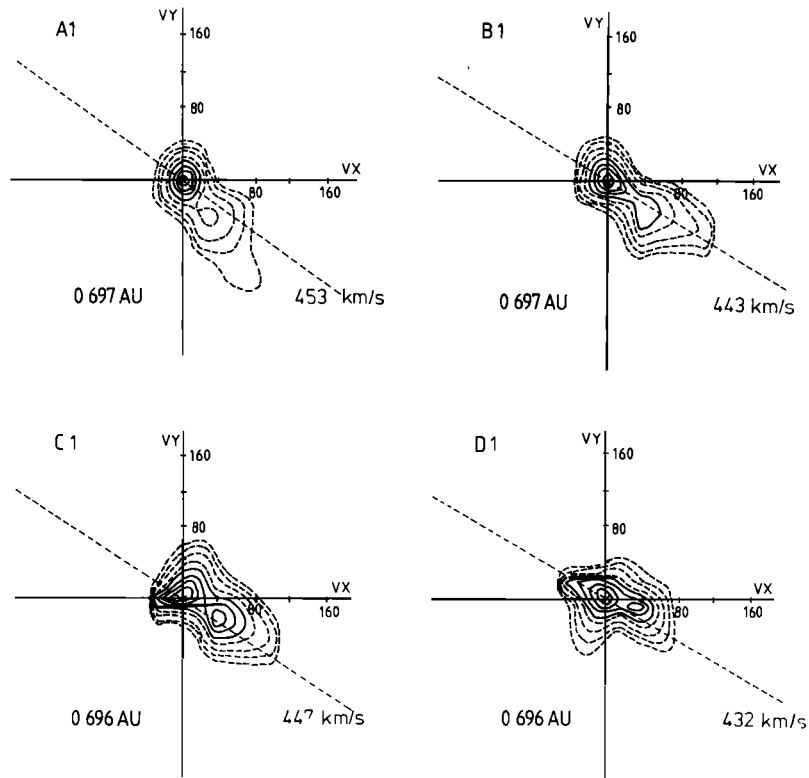


Fig. 3. Slow solar wind helium ion double peak distributions. The second component is drifting along the magnetic field direction with about the local Alfvén speed. Arrangement of the plots as in Figure 1. The corresponding plasma parameters are summarized in Table 1.

4. HELIOCENTRIC RADIAL TEMPERATURE DEPENDENCE

The Helios probes made it possible for the first time to determine average dependences of solar wind plasma parameters on solar radial distance from in situ measurements between 0.3 and 1 AU. In a preceding section nonthermal features of helium ion distributions were discussed, in particular the characteristics responsible for a temperature anisotropy. Here radial gradients of $T_{\parallel\alpha}$ and $T_{\perp\alpha}$ and consequently of the anisotropy $T_{\parallel\alpha}/T_{\perp\alpha}$ are examined in more detail.

We first should make some preliminary comments. For this study Helios 1 and 2 data were sorted into six different solar wind velocity classes for each of which averages over radial intervals of 0.1 AU width were computed. Thus the present study is limited in the sense that we have not determined the true gradients within a well-defined flux tube of a stream keeping its identity during the radial expansion. We cannot exclude the possibility that this averaging procedure sometimes mixes solar wind states that are not really comparable. Furthermore, the data set used here includes only the primary missions of the two Helios probes, during which the probes traversed only once the radial distance between 0.3 and 1 AU. Finally, as explained in section 3, the temperatures and the temperature anisotropies of helium ions were determined with less accuracy than those of the protons, and therefore a possible bias induced by the ion separation procedure cannot be ruled out completely.

In Figures 5a and 5b the temperatures $T_{\parallel\alpha}$ and $T_{\perp\alpha}$,

respectively, are shown versus radial distance from the sun on logarithmic scales. Power law indices (with an uncertainty of about 10–20%) for the radial dependence were obtained by least squares fits to the data. The different ranges of the

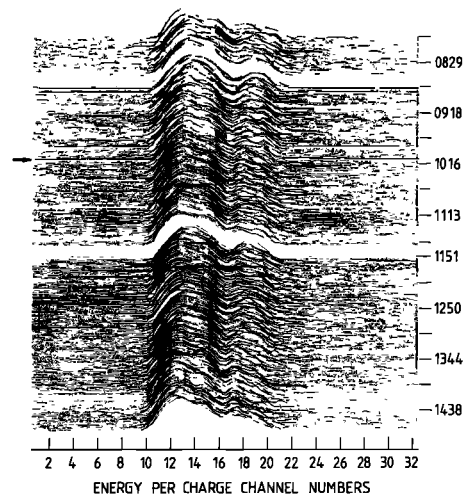


Fig. 4. Time series of combined E/q integrated ion count rate spectra starting on March 12, 1976, at 0831 UT and ending on March 12, 1976, at 1411 UT. Count rates are plotted logarithmically versus energy channel numbers except for the (0–5) count range. Note the stationary double peaked shape of the little ridge (He^{2+} distribution). Also the proton spectra exhibit a double humped shape (main ridge).

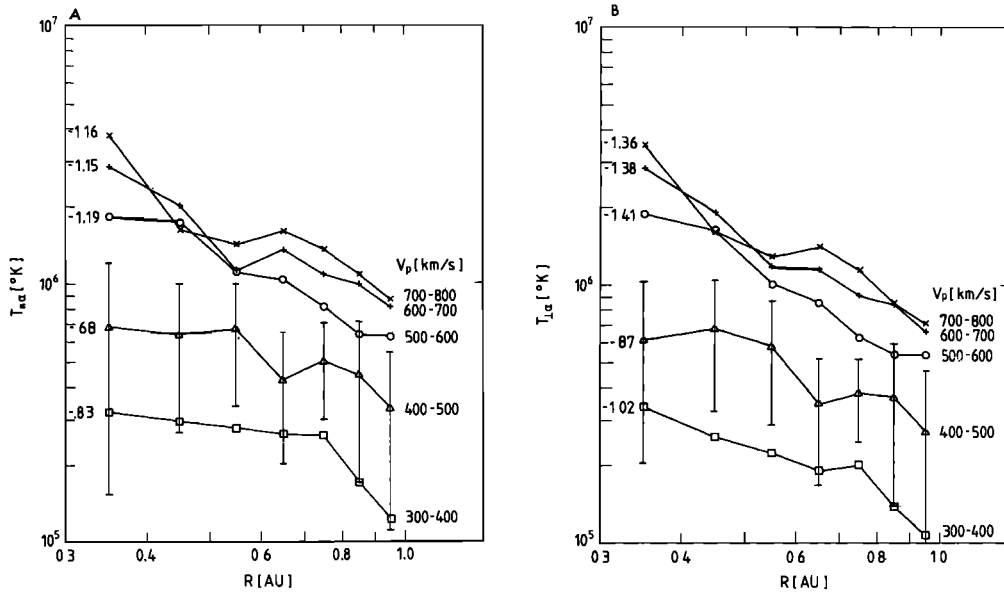


Fig. 5. (a) Average dependence of temperature $T_{||\alpha}$ on heliocentric radial distance in a double logarithmic plot for various ranges of the solar wind velocity. In the second curve from bottom mean square deviation bars are given that are also representative for the other curves. (b) Average dependence of temperature $T_{\perp\alpha}$ on heliocentric radial distance in the same format as in Figure 5a.

solar wind velocity are indicated in the figures at the right-hand side. Error bars indicating the mean square deviations of the individual points are shown on the curves corresponding to the velocity range between 400–500 km/s. These bars are also typical for the other curves. Examination of the Figures 5a and 5b shows that within the standard deviations no distinction is possible between the three upper curves. However, the differences between the low and high speed classes are significant because the uncertainties of the individual points amount to only a few percent. It can clearly be seen that at a fixed heliocentric distance the temperatures increase with increasing wind velocity. This observation is well known from measurements at the earth orbit [Feldman *et al.*, 1973, 1974a]. Furthermore, fast streams obviously exhibit steeper gradients, which means that fast helium ions appear to cool more rapidly than slow ones. The steepest decline with increasing solar distance is observed in high-speed wind for $T_{\perp\alpha}$, which goes as $T_{\perp\alpha} \sim R^{-1.38}$.

Because of the highly collisionless nature of the plasma in fast ion streams, there is basically no Coulomb coupling between parallel and perpendicular kinetic degrees of freedom (see Figure 13). Different temperature gradients for $T_{\perp\alpha}$ and $T_{||\alpha}$ are then most likely caused by waves that affect differently the particle velocity components parallel and perpendicular to the magnetic field. In fast streams the temperature $T_{||\alpha}$ goes roughly as $R^{-1.15}$. It is obvious from Figures 5a and 5b that the temperature profiles of slow and fast helium ion streams differ considerably. In slow wind the profiles are flatter: $T_{||\alpha} \sim R^{-0.75}$ and $T_{\perp\alpha} \sim R^{-0.94}$, indicating that heating occurs between 0.3 and 1 AU (heat conduction certainly plays a very minor role). As is shown in section 7 Coulomb collisions cannot be neglected in slow wind, where therefore collisional energy exchange with the protons probably has an important influence on the temperature of He^{2+} distributions.

Figure 6 demonstrates the average course of the anisotropy $T_{||\alpha}/T_{\perp\alpha}$ with heliocentric distance. For fast streams the points have been connected by straight lines to guide the eye. The error bar on the left-hand side indicates a typical mean square deviation of the individual points. Within the experimental uncertainties one can hardly draw any final conclusion from Figure 6 about the radial profile of the helium ion temperature anisotropy and its variation with the bulk speed. Nevertheless, the average radial trend in the data can be described as follows. Increasing anisotropies with increasing distance are in qualitative agreement with the physical picture that helium ions, moving in the diverging interplanetary magnetic field, tend to convert perpendicular into field-aligned kinetic energy. Within the large error bars $T_{||\alpha}/T_{\perp\alpha} \approx 1$, indicating nearly isotropic distributions in the perihelion, whereas $T_{||\alpha}/T_{\perp\alpha}$ had values of about 1.4 on the average at 1 AU. The points in Figure 6 corresponding to low-speed conditions are somewhat above those of high-speed wind. Thus the He^{2+} temperature anisotropy seems to be slightly larger in slow wind than in fast streams. It is recalled that for protons very different anisotropies and radial temperature profiles are observed [Marsch *et al.*, this issue].

Only sparse experimental background concerning radial dependences of helium ion plasma parameters has been available before now. Though the experimental errors are still large, the average radial gradients derived for $T_{||\alpha}$ and $T_{\perp\alpha}$ from Helios measurements provide further empirical material for theoretical work and may help to find better answers to the basic question of how wave-ion interaction establishes a dynamic equilibrium state of the solar wind. In this context it is interesting to compare the radial temperature profiles of the two ion species. There is a distinct contrast in the high-speed wind temperature profiles, where $T_{||\alpha}$ declines more rapidly with increasing radial distance

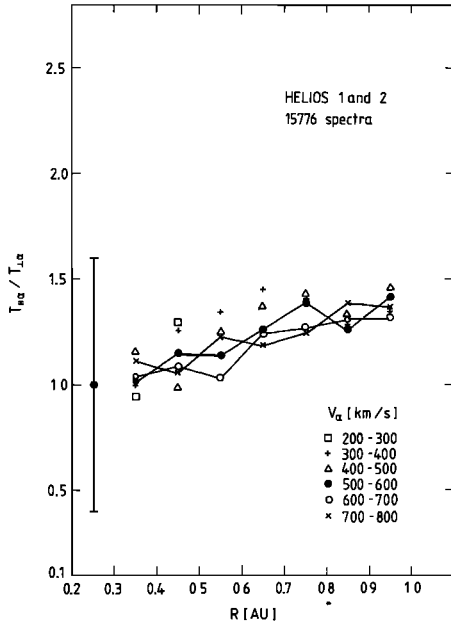


Fig. 6. Average dependence of the total helium temperature anisotropy on heliocentric radial distance for various ranges of solar wind velocity as indicated in the figure. Points represent averages over radial intervals of width 0.1 AU and have been partially connected to guide the eye. A typical mean square deviation bar is given on the left-hand side.

than T_{lp} . The reversed situation is met in low-speed wind where the protons seem to cool somewhat faster than helium ions during the wind expansion.

5. HELIUM AND HYDROGEN ION VELOCITY DIFFERENCES

This section is concerned with an investigation of helium and hydrogen ion bulk velocity differences $\Delta v_{\alpha p} = v_{\alpha} - v_p$ as observed by the Helios solar probes between 0.3 and 1 AU. Figure 7 presents Helios 2 observations from the primary mission during the time of solar activity minimum. Four successive solar rotations are shown. Below the panels the Carrington longitude, the time in days, the radial distance from the sun in AU, and the solar latitude are given. A similar plot with Helios 1 data is presented in the paper by Marsch *et al.* [1981a]. The first panel displays the solar wind velocity v_p (proton bulk speed), the second gives the differential speed $\Delta v_{\alpha p} = |\Delta v_{\alpha p}|$. This quantity was multiplied by a minus sign if $v_p > v_{\alpha}$ in order to indicate times when the helium speed was below that of the protons. But this was done only in low-speed wind with $v_p \leq 400$ km/s. Namely, that there were also found several time periods in fast streams, when $v_p > v_{\alpha}$. However, in these cases $\Delta v_{\alpha p}$ has not been multiplied by a minus sign, because $\Delta v_{\alpha p} \neq 0$ during a drastic directional change of \mathbf{B} . In contrast, in slow plasma a sign reversal of $\Delta v_{\alpha p}$ usually corresponded to $|\Delta v_{\alpha p}|$ actually going through zero. For comparison, the Alfvén speed v_A has been indicated by points in Figure 7. The Alfvén speed is calculated by using the total ion mass density: $v_A = B / (4\pi(n_p m_p + n_{\alpha} m_{\alpha}))$. The last panel shows the scalar product between the unit vectors of the magnetic field \mathbf{B} and $\Delta \mathbf{v}_{\alpha p}$, which is equal to the cosine of the angle they form.

Inspecting the upper and middle panel of Figure 7 the

observations can be summarized as follows: helium and hydrogen ions in the solar wind typically exhibit bulk speed differences at all radial distances between 0.3 and 1 AU. In very low-speed wind, He ions tend to stay behind the protons by some kilometers per second. With increasing solar wind speed the situation becomes reversed and in the body of high-speed streams most of the time the helium ion velocity exceeds that of the protons considerably. At a fixed radial distance the solar wind speed may serve as an ordering parameter to characterize differential ion velocities as has been done already by Asbridge *et al.* [1976].

For solar wind of a given speed at various radial distances, a clear tendency is visible in the Figure 7 for an absolute increase of $\Delta v_{\alpha p}$ in high-speed streams with decreasing distance from the sun. However, in low-speed wind no pronounced and systematic variation in the differential velocity as a function of radial distance has been observed. Comparing the local Alfvén speed (indicated by points) with the ion differential speed, a similar shape for the profiles of $\Delta v_{\alpha p}$ and v_A is found. The Alfvén speed seems to present an upper limit for $\Delta v_{\alpha p}$ which is sometimes attained in very fast plasma [Marsch *et al.*, 1981a]. Note that near perihelion (period at day 105 to day 110) both velocities agree remarkably well within experimental errors despite large fluctuations. It appears from these figures that $\Delta v_{\alpha p}$ reaches its upper limit v_A more easily closer to the sun.

The field alignment of the vector $\Delta \mathbf{v}_{\alpha p}$ is confirmed by the observations presented in the last panel of Figures 7. Here it is shown that the relative motion of the two ion species is along the local magnetic field direction. This has been observed earlier at 1 AU by Asbridge *et al.* [1976]. Ideally, the cosine should be plus or minus one according to the general polarity of the magnetic sector. In high-speed wind where the direction of $\Delta \mathbf{v}_{\alpha p}$ is well defined by the measurement there is an excellent agreement with the simultaneously measured magnetic field direction. Depending on the magnetic polarity in fast streams the cosine is nearly exactly ± 1 . In middle or low-speed regions the vector correlation is not so convincing. Higher directional uncertainties of the measured $\Delta \mathbf{v}_{\alpha p}$ arise because this vector fluctuates around zero in slow plasma.

Some evidence may be found in Figure 7 for the occurrence of very pronounced differential speeds right at the leading edges of high speed streams [Hirschberg *et al.*, 1974]. Note for example the data at about days 38, 48, 57, and 74. This finding may be connected to the observation that wave pressure forces are strongest in correlation with highest wave activity at the time of a high-speed stream onset [Morfill *et al.*, 1979; Denskat *et al.*, 1981]. We emphasize that for the time period under discussion the magnetic field fluctuations $\delta \mathbf{B}$ and proton bulk velocity fluctuations δv_p are closely correlated in high speed streams, which suggests that they are Alfvén type waves. The existence of Alfvén waves in the solar wind was shown by Belcher and Davis [1971] and for the data set used here also by Denskat *et al.* [1981].

In order to illustrate the occurrence of Alfvén fluctuations in Figure 8, six hours of Helios 2 observations are shown as obtained in a high-speed stream ($v_p \approx 700$ km/s) at 0.75 AU on day 66 in 1976. Reading from above the azimuthal and subsequently the elevation angles of the proton and helium

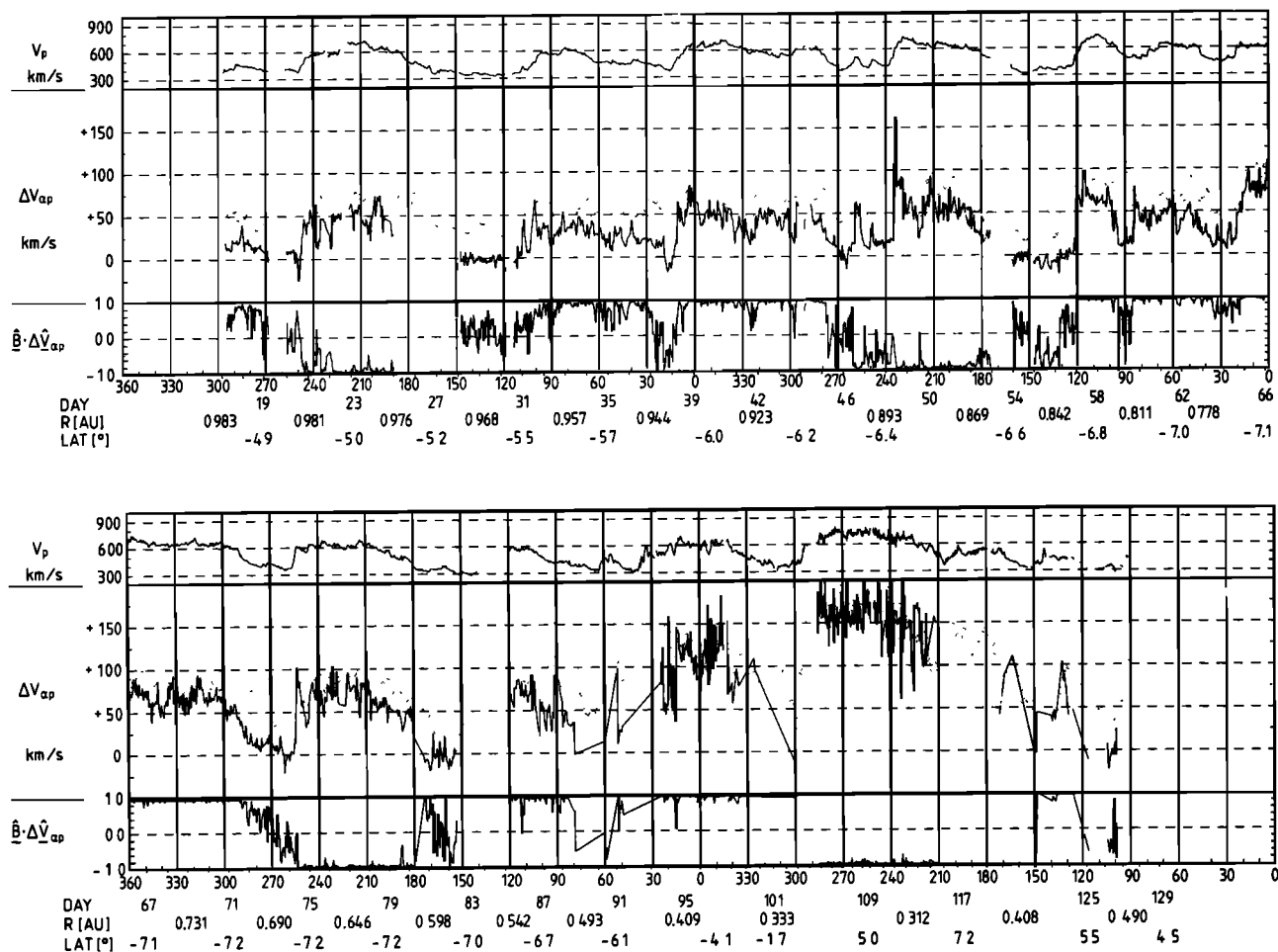


Fig. 7. One-hour averages of proton bulk velocity, ion differential speed $\Delta v_{ap} \cdot \text{sign}(|v_{\alpha}| - |v_p|)$, and the scalar product between the unit vectors of magnetic field and Δv_{ap} versus Carrington longitude for four successive solar rotations. Data shown have been obtained by Helios 2 between January 17, 1976, and May 3, 1976, while the solar probe traversed a radial distance between 1.0 and 0.3 AU. The Alfvén velocity is indicated by points in the second panel. The distinct sign reversals in the last panel indicate the crossing of a magnetic sector boundary.

ion bulk velocity and the magnetic field vectors are given. Directional fluctuations in v_p and \mathbf{B} are obviously inversely correlated, as can be inferred from the first and third and from the fourth and sixth panels. Enormous fluctuations in ϵ_B occur that range from plus to minus 45° and that have their counterparts in ϵ_p , but with a smaller amplitude. At about 0900, 0930, 1040, and 1100 UT marked changes in α_B appear, with deviations from the average value in the range from -40° to more than $+90^\circ$. Corresponding changes of α_p are simultaneously observed. Similar drastic changes of the magnetic field direction have been measured earlier by the earth bounded Heos 2 satellite and have been studied with respect to their influence upon the ion bulk velocities by H. Grünwaldt and H. Rosenbauer (private communication, 1980). Note that the helium ion flux angles in Figure 8 do not exhibit fluctuations similar to the protons but are fairly constant with average values close to zero. The helium ions seem to stream radially away from the sun, whereas the protons are heavily disturbed by Alfvénic type wave activity as indicated by the angular correlation of fluctuations in v_p and \mathbf{B} . The picture emerges of the minor ions 'surfing' on the

waves which are carried by the protons.

This conclusion is supported by Figure 9, in which from top to bottom the proton bulk speed (with the helium ion bulk speed indicated by points), the ion differential speed Δv_{ap} and finally $\hat{\mathbf{B}} \cdot \Delta \mathbf{v}_{ap}$ are displayed. The first panel demonstrates that the helium ion speed v_α is fairly constant, which—in connection with the flux angles shown in Figure 8—means that the constant vector v_α is permanently directed radially away from the sun. In contrast, owing to wave activity, the proton bulk velocity v_p fluctuates in direction and amplitude. The middle panel shows that in spite of fluctuations the differential speed Δv_{ap} is close to the Alfvén speed (v_A is marked by points). The directions of v_p and \mathbf{B} are highly variable, but the differential speed vector Δv_{ap} is remarkably well aligned with \mathbf{B} , as is clearly shown in the last panel of Figure 9. In the time intervals around hour 0930 and 1040 when $\alpha_B > 90^\circ$, the vector Δv_{ap} was also pointing back to the sun. The alpha particles appeared to move slower than the protons ($v_p > v_\alpha$), but Δv_{ap} did not go through zero but simply turned around following the magnetic field direction. Obviously, in connection with Alfvénic

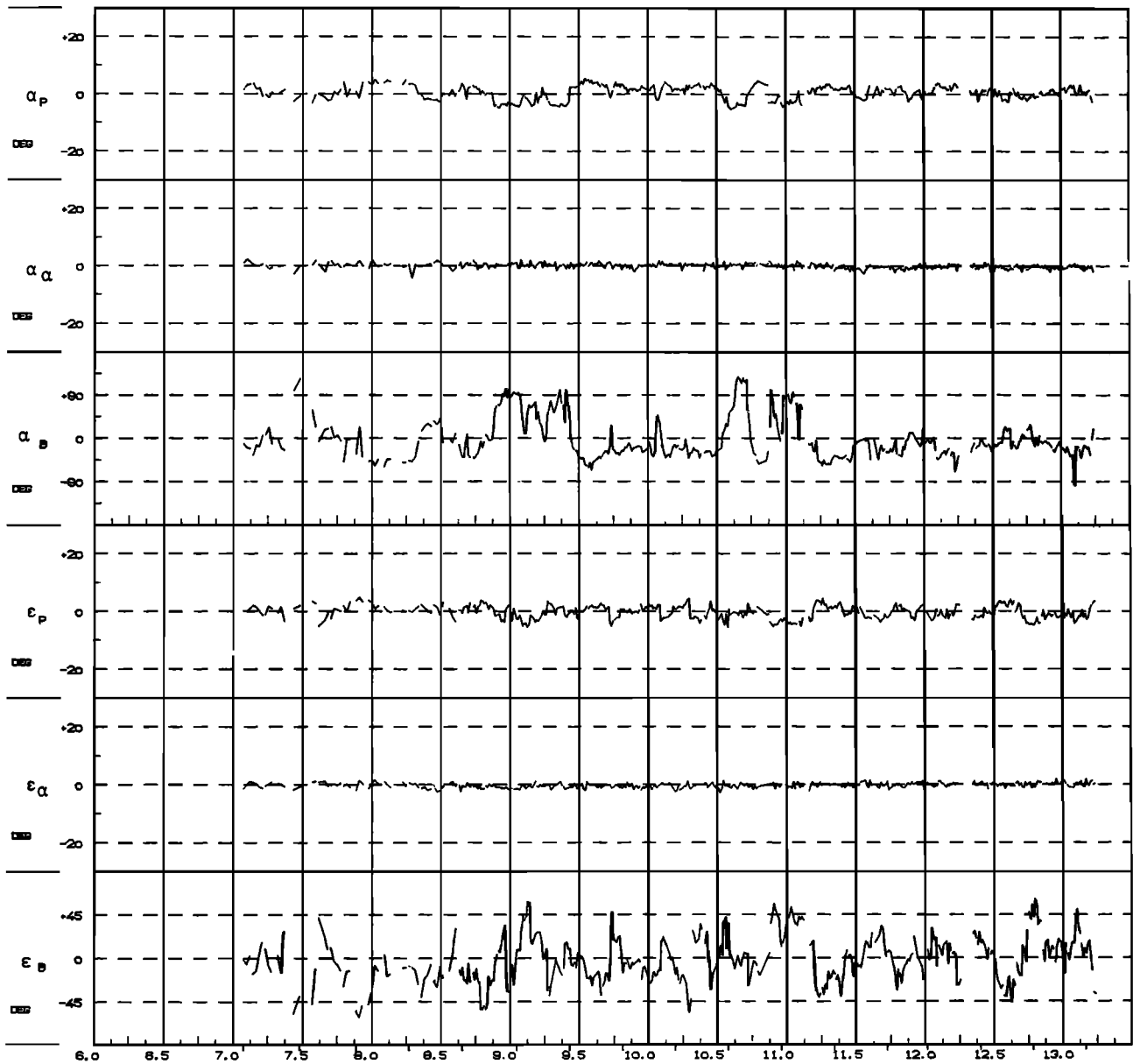


Fig. 8. Six hours of Helios 2 data measured at day 66 in 1975 at 0.75 AU. Reading from above, the azimuthal and elevation angles are shown for the proton and helium ion bulk velocity and the magnetic field vector.

fluctuations kinks can occur in the magnetic field lines that appear as polarity reversals of short duration (see again Figure 8). During these time periods the proton heat flux was also pointing back to the sun [Marsch *et al.*, this issue]. Similar observations made at 1.0 AU have been reported by Grünwaldt and Rosenbauer [1980]. This phenomenon was extensively described in order to emphasize the contrast to the situation in very low-speed wind when usually Δv_{ap} is directed towards the sun and the helium ions actually lag behind the protons over extended time periods.

The radial dependence of the ion differential velocity is shown by Figure 10. For five solar wind velocity classes, averages of Δv_{ap} have been performed over the data sorted into radial intervals of 0.1 AU width. The corresponding mean values have been plotted in the middle of the respective intervals. There is on the average a very low differential velocity between the two ion species in a solar wind with

speed ranging from 300 to 400 km/s. (The lowest velocity class, less than 300 km/s, couldn't be shown as such low velocity values have only been observed for some short time periods near the perihelion). Also, no clear radial dependence of Δv_{ap} can be detected for the slow solar wind ($v_p \leq 400$ km/s). It is obvious in Figure 10 that at a fixed radial distance from the sun an increase of solar wind speed is on the average accompanied by an increasing differential speed. This effect is most pronounced in the perihelion at 0.3 AU, where average velocity differences up to 150 km/s are found. In high-speed streams Δv_{ap} exhibits a distinct increase with decreasing heliocentric distance.

Figures 7 and 9 have illustrated the observation that with increasing solar wind speed the differential ion velocity tends to approach the local Alfvén velocity. This result is further emphasized in Figure 11, which presents frequency of occurrence histograms for slow, intermediate speed, and fast solar

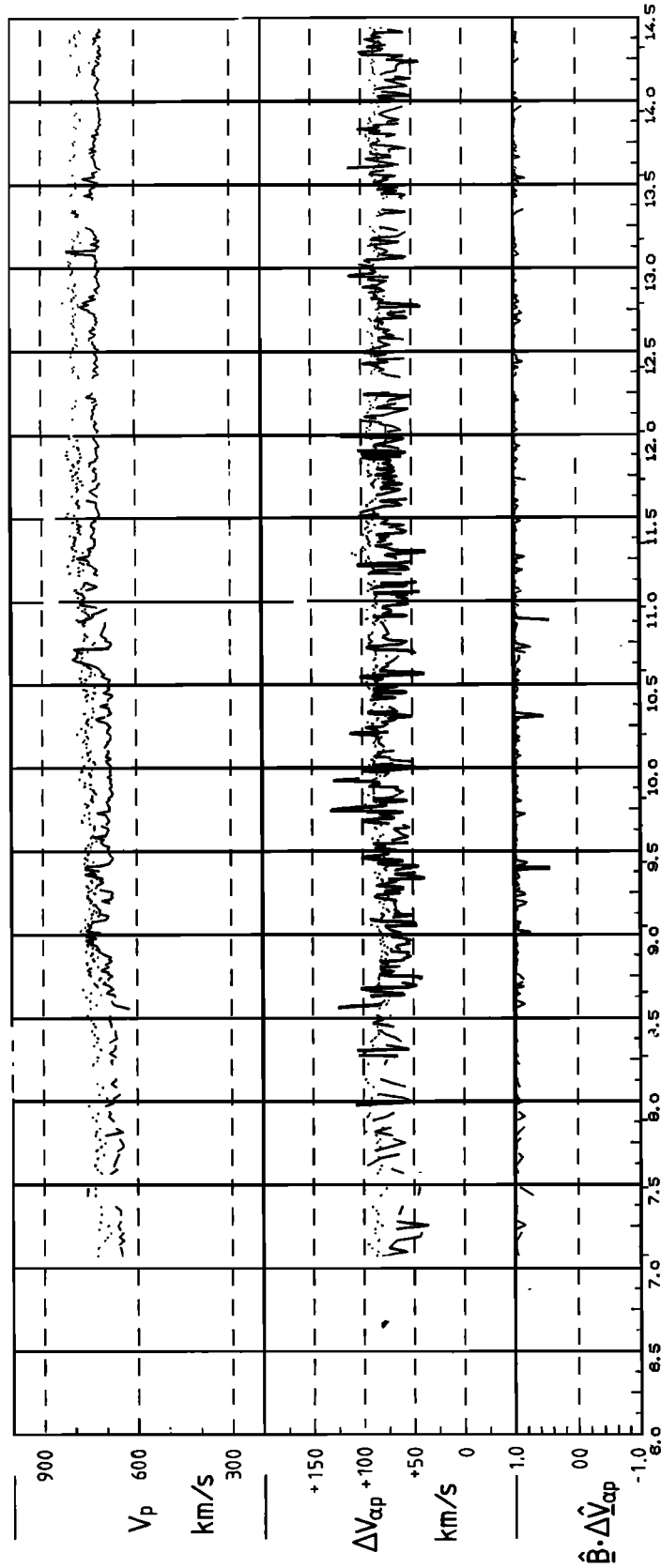


Fig. 9. Six hours of data as obtained by Helios 2 at 0.75 AU on day 66 in 1976. From top to bottom the proton bulk speed (solid line) and the helium ion bulk speed (dotted line), the ion differential speed (v_A is marked by points), and finally the scalar product $\hat{B} \cdot \Delta \hat{V}_{cp}$ are displayed.

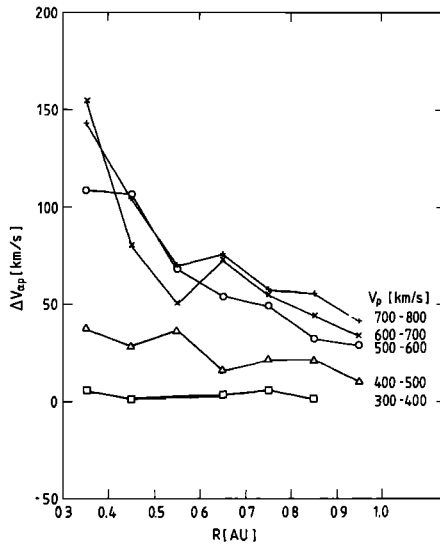


Fig. 10. Ion differential speed $\Delta v_{ap} \cdot \text{sign}(|v_\alpha| - |v_p|)$ versus heliocentric radial distance for various regimes of solar wind velocity as indicated at the curves. Average values have been calculated for radial intervals of width 0.1 AU and plotted in the middle of the corresponding intervals. Points are connected by straight lines to guide the eye.

wind. The number of cases where Δv_{ap} attained certain percentages of v_A are shown. Clearly visible is the tendency for the right-hand hump in each distribution to become peaked around higher percentages of v_A with increasing wind velocity. The differential ion speed reaches on the average 80% of v_A in the body of fast streams with $v_p > 600$ km/s. However, the corresponding distribution is fairly broad and includes also cases, in which $\Delta v_{ap} \approx v_A$ is observed.

An unexpected feature in Figure 11 is the double humped shape of the frequency distributions, with a clear separation at zero. In low-speed wind ($v_p < 400$ km/s) the area under the left-hand distribution is comparable to that under the right-hand distribution. A nearly equal probability of He^{2+} being slightly slower or slightly faster than protons is observed. With increasing speed the left hump decreases in relative

size, whereas the right-hand distribution becomes most pronounced. From a theoretical point of view, one would expect the left distribution if no preferential acceleration of He^{2+} ions were occurring in the solar wind. Namely, the helium ions, because of their different mass per charge ratio, feel only half the interplanetary electrostatic force experienced by the protons and thus fall behind them during the solar wind expansion. (Compare with older solar wind models: *Geiss et al.* [1970]). As far as the right-hand part of the frequency distributions is concerned, the observation of pronounced differential velocities, which at 0.3 AU can be as much as 25% of the proton bulk speed, represents a serious challenge to future detailed solar wind expansion theories and the particle acceleration mechanism involved.

The observed close correlation between v_A and Δv_{ap} presents evidence that Alfvén waves or waves with comparable phase velocity may accomplish the preferential acceleration of the helium ions with respect to protons. This has been proposed by *Hollweg* [1974], *Hollweg and Turner* [1978], and *McKenzie et al.* [1979]. At larger distances the differential speed reaches the local Alfvén speed more seldom, even under high speed conditions. This may be due to the declining power of the waves for larger radial distances [*Behannon*, 1976] or because Coulomb and rotational forces may become more effective [*McKenzie et al.*, 1979]. Another reason may be that v_A represents only a gross order parameter because field-aligned waves exist in the solar wind with a fairly broad phase velocity spectrum. Thermal anisotropies in the proton and electron distributions also considerably change the phase velocities of waves in the framework of kinetic plasma theory with respect to the MHD cold plasma limit.

One may tentatively interpret the right hump in the distribution for low speeds (left column) in Figure 11 as being due to preferential acceleration caused by temporarily intense wave activity even in slow solar wind. This possibility has been overlooked in previous works on this topic. In a separate paper [*Marsch et al.*, 1981b] a clear example of pronounced differential ion speeds obtained in slow solar wind near the Helios 2 perihelion during the time of increasing solar activity will be presented.

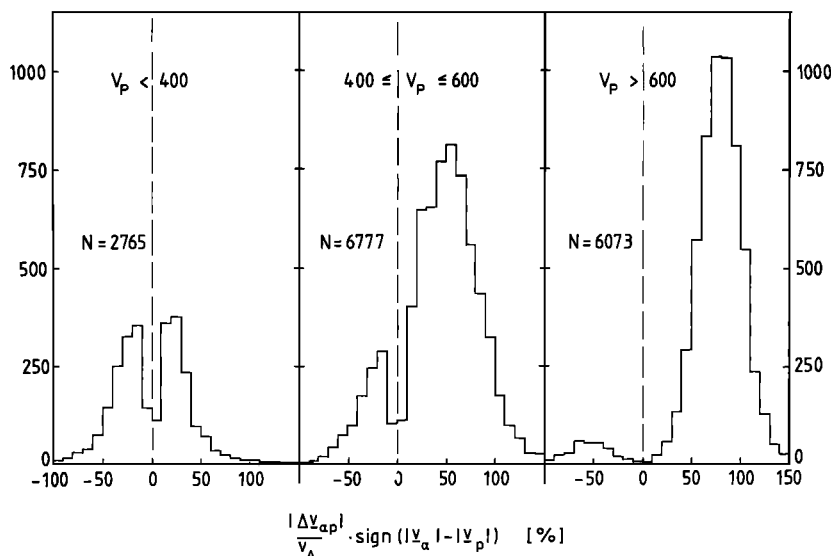


Fig. 11. Histograms of the ion differential speed in percentage of the local Alfvén speed for low, intermediate, and high-velocity streams.

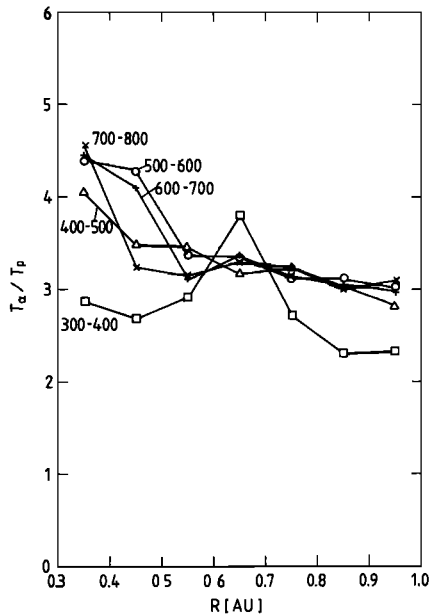


Fig. 12. Average dependence of the ratio of helium ion to proton temperature on solar radial distance for different regimes of solar wind speed.

The left-hand distribution in the high speed column of Figure 11 may be attributed to occasionally occurring magnetic field reversals of the type shown in Figure 8, which give rise to $v_p > v_\alpha$ by rotating $\Delta v_{\alpha p}$ back toward the sun. These cases most likely make up the left hump in the high speed distribution of Figure 11 and also partly in the intermediate speed one, which corresponds to the leading and trailing edges of fast streams and stream interaction regions.

6. HELIUM AND HYDROGEN TEMPERATURE RATIO

From observations at 1 AU it has been known for a long time that considerable temperature differences between the various ion species exist in the solar wind. The ratio of helium to hydrogen ion temperatures reported from different spacecraft observations ranges from about 2 up to 5–6, [Feldman *et al.*, 1974a; Neugebauer, 1976, 1981; Feynman, 1975]. In this section mean temperatures are used that are defined for helium (and equally for the protons) by one third of the trace of the temperature tensor or equivalently by $T_\alpha = (T_{\parallel\alpha} + 2 T_{\perp\alpha})/3$. In Figure 12 the measured ratio T_α/T_p is shown versus radial distance from the sun for various solar wind velocities. All helium spectra available from the primary missions of both Helios probes have been sampled. Mean values of T_α/T_p falling into intervals of 0.1 AU width are plotted in the middle of the corresponding intervals.

Some qualitative trends can be inferred from Figure 12. The lowest temperature ratios are obtained for all radial distances in slow plasma ($v_p < 400$ km/s). The larger values at about $R = 0.6$ AU may be an artifact caused by insufficient statistics (see corresponding comments in section 4). For high-speed wind a definite increase of T_α/T_p from about 3 at 1 AU to 4.5 at 0.3 AU can be seen. Figure 12 also shows that in intermediate and slow speed solar wind ($v_p \leq 500$ km/s) the temperature ratio basically exhibits no radial gradient; average values lie between 2 and 3.5. On the other hand in fast streams ($v_p > 500$ km/s) on the average helium ions appear to cool somewhat faster than protons during the solar

wind expansion from 0.3 to 1.0 AU. This can be concluded from the decrease of T_α/T_p with increasing heliocentric distance. (See again section 4 for the radial gradients of $T_{\parallel\alpha}$ and $T_{\perp\alpha}$. For the corresponding proton parameters refer to Marsch *et al.* [this issue].) One can recognize a kind of a kink in the curves at about 0.5–0.6 AU, inside of which the gradient steepens with decreasing solar distance. Average values of T_α/T_p about 4 or even larger are mainly observed near the perihelion, whereas for $R \geq 0.6$ AU the temperature ratio T_α/T_p varies between 3 and 3.5. This means that strongest relative cooling of the helium with respect to hydrogen ions with increasing heliocentric distance seems to occur in the radial interval between 0.3 and 0.6 AU according to Helios observations.

We recall that the observed radial ion temperature profiles are flatter than one would expect for adiabatic cooling. Thus a yet still unknown heat source has to be invoked in order to explain why the temperatures are maintained above an adiabatic value. Owing to the results presented in Figure 12 one may reverse the previous arguments and conclude that it is basically inside 0.5 AU where in high speed wind the helium ions are preferentially heated, with the strength of the heating source becoming greater closer to the sun. Barnes and Hung [1973] have investigated the influence of dissipation of hydromagnetic waves on T_α/T_p and found that helium might be heated more than hydrogen by this mechanism. Because wave activity generally grows with decreasing solar distance [Denskat *et al.*, 1981; Behannon, 1976], the strongest preferential heating should occur close to the sun. The observations of T_α/T_p in Figure 12 should be considered in close connection with the finding that the largest differential velocities between the two ion species have been observed near 0.3 AU as discussed in the preceding section. Similar ideas have recently found strong support from satellite data at 1 AU by Neugebauer and Feldman [1979] who established an empirical linear relationship between $\Delta v_{\alpha p}$ and T_α/T_p . The most important aspect of these results in our opinion is that possibly a not yet well understood common physical process in fast streams exists, which is responsible for both preferential minor ion heating and acceleration, thereby causing the observed close correlation of T_α/T_p with $\Delta v_{\alpha p}$. While we do not know very much in detail about the possible wave heating and acceleration processes, the plasma measurements can be used for an investigation of the frictional action of Coulomb collisions, and so at least this aspect of the problem can be clarified. Therefore in the following section we will consider the influence of Coulomb friction on $\Delta v_{\alpha p}$ and T_α/T_p and study the possible collisional limitation of these quantities between 0.3 and 1 AU.

7. THE ROLE OF COULOMB FRICTION IN LIMITING T_α/T_p AND $\Delta v_{\alpha p}$

The relevant time scales for energy ($\tau_{\alpha p}$) and momentum exchange (τ_s) between colliding ions have been evaluated by Spitzer [1962]. They have to be compared with the solar wind expansion time scale $\tau_{\text{exp}} = [-v_p(d/dR) \ln n_p]^{-1}$ which gives $\tau_{\text{exp}} \equiv R/2v_p$ for a density profile $n_p \sim R^{-2}$, which represents a sufficient fit to the measurements. Complementing the previous investigations by Feldman *et al.* [1974a] and Neugebauer [1976] at 1 AU, the present study utilizes data from the whole radial interval between 0.3 and 1 AU. Taking the slight dependence of the so-called Coulomb logarithm on

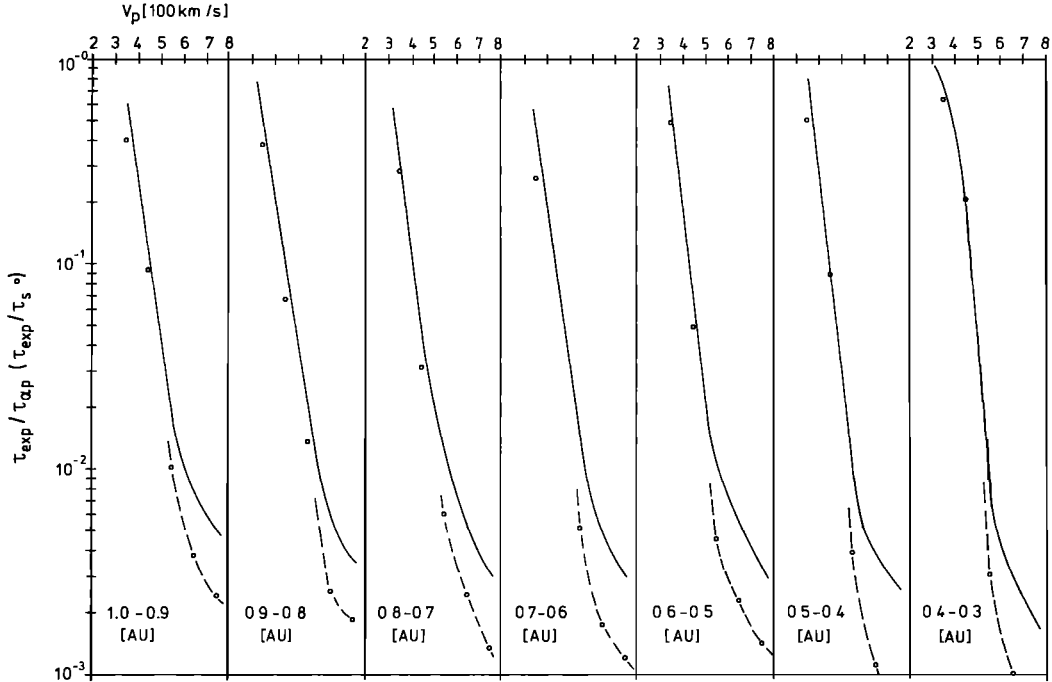


Fig. 13. Ratio of solar wind expansion time to collisional energy exchange time versus proton bulk speed as calculated from Helios 1 and 2 plasma measurements at various radial distances. Dashed line shows the ratio of the expansion time to the collisional slowing down time.

radial distance into account, the time for equalization of the two ion temperatures [Spitzer, 1962] may be written for the present purpose in the form:

$$\tau_{\alpha p} = 5.87(T_p + T_\alpha/4)^{3/2}/(n_p(9.15 + 1.5 \ln T_p - 0.5 \ln n_p))$$

where the proton density n_p is given in cm^{-3} and the mean temperature T_α and T_p are given in degrees Kelvin. The slowing down time for helium test particles in the proton plasma due to multiple small angle deflections [Boyd and Sanderson, 1969] is

$$\tau_s = 9.35 T_p^{3/2}/(n_p(9.15 + 1.5 \ln T_p - 0.5 \ln n_p)) \cdot F(x)$$

The brackets contain the Coulomb logarithm written out explicitly. Here elementary constants have already been replaced by their numerical values. The function $F(x) = 4x^3/[3\sqrt{\pi}(\phi(x) - x\phi'(x))]$ is determined by the error function $\phi(x)$ and its derivative $\phi'(x)$ and fulfils $F(0) = 1$. The argument x is the test particle velocity with respect to the frame of the background protons in units of their thermal speed. To take the differential velocity $\Delta v_{\alpha p}$ into account, which can be larger than both ion thermal speeds, we have used $x = ((k_B T_\alpha + m_\alpha \Delta v_{\alpha p}^2/3)/(4k_B T_p))^{1/2}$ (k_B is Boltzmann's constant) as a typical value for the normalized helium test particle speed. The $\Delta v_{\alpha p}$ term leads to essential corrections in high-speed plasma.

In Figure 13 the ratio of $\tau_{\text{exp}}/\tau_{\alpha p}$ and τ_{exp}/τ_s are plotted versus the proton bulk velocity for various radial intervals. Average ratios have been calculated from the measured moments according to the formulae presented above for proton bulk velocity intervals 100–200 km/s, 200–300 km/s, etc. Continuous lines correspond to $\tau_{\text{exp}}/\tau_{\alpha p}$, whereas circles and dashed lines indicate τ_{exp}/τ_s . Deviations in the course of both curves are obtained at solar wind velocities larger than 500 km/s, reflecting the pronounced ion differential speeds

measured in high-speed streams. The steep decline of all curves illustrates the drastic decrease of Coulomb friction with increasing solar wind velocity. More than two orders of magnitude difference separate the values for slow and fast plasma with a slight tendency of these differences to become even larger closer to the sun. Thus high-speed streams are characterized by Coulomb collisions being practically negligible due to the high-temperature, low-density conditions. The observed ion differential velocity, whatever may cause it, once being established still further reduces the effective Coulomb friction between the two ion species. On the other hand, in slow plasma of less than 300 km/s a thermal helium ion suffers at least one impact while travelling through a typical density scale height of length $R/2$ at the radial distance R .

One normally speaks of a plasma being Coulomb collision dominated if the ratio of mean free path to scale height is substantially less than one. Our analysis has been done for thermal particles. Strictly speaking, the slowing down and energy exchange times are functions of the relative velocity of two colliding ions in the solar wind frame. Thus particles with velocities less than the thermal speed are more strongly affected by collisions than, say, protons in a beam component. Taking the velocity dependence of $\tau_{\alpha p}$ or τ_s into account exactly would have required basing the study on the detailed distribution functions. That would necessarily have complicated the investigation. However, our analysis yields good first-order approximations and may still lead to the conclusion that in slow solar wind the influence of Coulomb collisions cannot be neglected. For high-speed streams Figure 13 furthermore clearly demonstrates that because of extremely small values of τ_{exp}/τ_s between 0.3 and 1 AU, anomalous collision processes due to wave-particle interactions have to be invoked to explain isotropisation processes as they are actually observed in the ion distributions. In

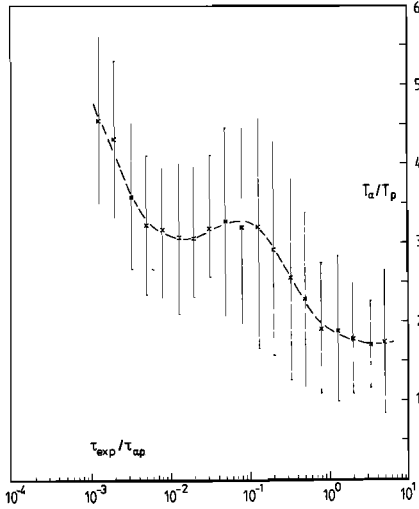


Fig. 14. Observed helium to hydrogen temperature ratio versus the ratio of solar wind expansion time to temperature equalization time as calculated from the measurements. Averages of T_α/T_p have been performed for finite intervals of the time ratio, and error bars indicate the corresponding mean square deviations.

order to understand the effective frictional coupling between the two ion species a thorough knowledge of the wave-particle interactions in the solar wind on a microscopic scale is thus urgently required.

The dependence of the measured temperature ratio on $\tau_{\text{exp}}/\tau_{\alpha p}$ is illustrated in Figure 14, where mean values of T_α/T_p (crosses) and their mean square deviations (error bars) are shown. The T_α/T_p values have been sorted into equally spaced intervals of $\tau_{\text{exp}}/\tau_{\alpha p}$ on a logarithmic scale extending from 10^{-4} to 10^1 . The observed T_α/T_p ratio ranges from 4.5 in the collisionless limit to 1.7 in case of a few collisions during a solar wind expansion time interval. Clearly, Figure 14 does not establish a causal relationship but simply classifies observed T_α/T_p values according to the corresponding 'local' plasma conditions characterized by $\tau_{\text{exp}}/\tau_{\alpha p}$. Note that within the large error bars $T_\alpha/T_p \approx 1.7$ for $\tau_{\text{exp}}/\tau_{\alpha p} > 1$. Under these conditions, corresponding to slow, cold, dense wind, Coulomb collisions still appear to be important in limiting T_α/T_p . But even then this ratio is not equal to one, which would indicate thermal equilibrium. However, within the error bars the observed points are consistent with a linear dependence of T_α/T_p on $\tau_{\text{exp}}/\tau_{\alpha p}$ that passes through $T_\alpha/T_p = 1$ for values of $\tau_{\text{exp}}/\tau_{\alpha p}$ larger than 10. One should be aware of this point in the following somewhat speculative discussion. The average temperature ratio T_α/T_p is observed to have a nearly constant value of 3.2 for $\tau_{\text{exp}}/\tau_{\alpha p}$ between 3×10^{-3} and 10^{-1} . From Figure 13 one can recognize that this parameter range is characteristic of the leading and trailing edges of fast streams and stream interaction zones for the time period under discussion in this paper. It is possible that bulk flow inhomogeneities and stream merging may significantly raise the He^{2+} temperature with respect to the proton temperature in these regions, though in a yet unknown way. However, values of $T_\alpha/T_p > 4$ belong to pure high-speed states with $v_p \geq 600$ km/s (see also Figure 13). Because highest $\Delta v_{\alpha p}$ values are also observed under these conditions, it may be concluded that in these cases microscopic resonant or macroscopic nonresonant wave-particle interactions are responsible for

the preferential helium heating and acceleration forces which can not be counterbalanced by collisional friction.

It is noteworthy that generally the temperature ratio determined from Helios measurements is slightly smaller than was previously published in the literature [Asbridge *et al.*, 1976; Neugebauer, 1981]. In addition, the 'plateau' in Figure 14 at $T_\alpha/T_p \sim 3.2$ has not been previously reported. The plateau would mean that T_α/T_p is on the average essentially independent of the proton bulk speed in the range from roughly 400 to 600 km/s. These results are in qualitative agreement with Prognost 1 observations from 1 AU by Bosqued *et al.* [1976]. We do not want to overemphasize this finding. Because of the large error bars in Figure 14, its statistical significance may be questionable. For very fast streams ($v_p > 700$ km/s) and slow wind ($v_p < 350$ km/s) both T_α/T_p and $\Delta v_{\alpha p}$ vary inversely with $\tau_{\text{exp}}/\tau_{\alpha p}$ and τ_{exp}/τ_s , respectively. This agrees with the positive correlation between T_α/T_p and $\Delta v_{\alpha p}$ already reported on the basis of earth satellite results by Neugebauer and Feldman [1979]. However, Helios observations indicate that this positive correlation holds only for 'pure' high and 'pure' low-speed wind. In our opinion, this correlation seems to be of physical significance only in slow plasma where the 'local' collisions may really be able to control T_α/T_p and $\Delta v_{\alpha p}$ because $\tau_{\text{exp}}/\tau_{\alpha p} \approx 1$ and $\tau_{\text{exp}}/\tau_s \approx 0.5$. For intermediate speed wind, macroscopic stream interaction phenomena may also play a prominent role in limiting the ion temperature ratio.

In Figure 15 the results of a similar analysis as above are displayed in order to demonstrate the possible limitation of $\Delta v_{\alpha p}$ by Coulomb collisions. The absolute value of $\Delta v_{\alpha p}$ times the sign of the difference between the bulk velocity magnitudes of the two ion components is shown versus the ratio of solar wind expansion time to the test particle slowing down time τ_{exp}/τ_s . For intervals of the ion differential velocity of width 10 km/s in the range of -50 to $+150$ km/s, the corresponding τ_{exp}/τ_s mean values have been calculated. Sorting $\Delta v_{\alpha p}$ values into different τ_{exp}/τ_s intervals was not suitable for our investigation because positive and negative differential velocities would have been mixed together, which now form two different branches of the curve in Figure 15.

The negative branch was found for the first time in a study

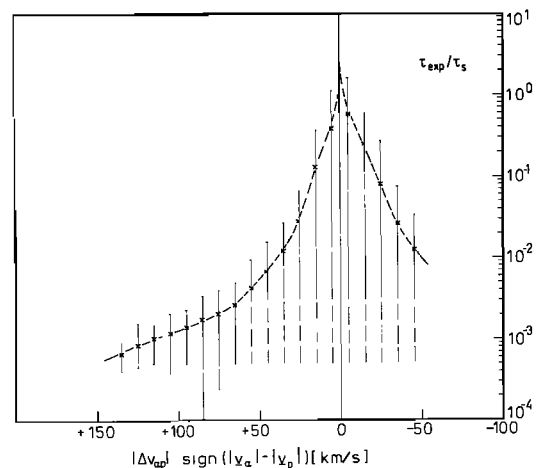


Fig. 15. Observed ion differential speed displayed versus the simultaneously calculated ratio of solar wind expansion time to particle collisional slowing down time. Note the two branches, where largest $|\Delta v_{\alpha p}|$ values correspond to high-speed streams.

by Grünwaldt and Rosenbauer [1978], though it had long been known that in slow plasma helium ions tend to lag behind the protons [Asbridge *et al.*, 1976]. In Figure 15 the largest negative differential speeds of about -50 km/s pertain to values of $\tau_{\text{exp}}/\tau_s \approx 10^{-2}$. The corresponding data were obtained in high-speed regions in which the helium ions were temporarily observed to move slower than the protons. This point was discussed extensively in section 5. It is clear that the largest fluctuations in Δv_{ap} should be expected under high-speed conditions when the Coulomb friction is negligible. If in that case a preferential acceleration mechanism is absent, the protons are unable to drag the helium ions with them via binary collisions. On the other hand, under the influence of a selective acceleration source the helium and hydrogen plasma components can interpenetrate each other like two frictionless, ideal liquids. The part farthest to the left of the positive branch in Figure 15 (consisting mainly of data collected in very fast plasma near 0.3 AU) corresponds to such conditions. In contrast, note that nearly vanishing differential speeds are observed when collisions are thought to be playing a role. This is expressed by the triangular form of the curve in the region around $\tau_{\text{exp}}/\tau_{ap} \approx 0.1-1.0$, where $\Delta v_{ap} \approx 0$. Similar results from earth-bound satellites have been published by Grünwaldt and Rosenbauer [1978] and collected in a recent review paper by Neugebauer [1981]. Thus under typical slow wind conditions Coulomb collisions may still effectively limit Δv_{ap} .

8. SUMMARY AND CONCLUSIONS

This study dealt with helium ion three-dimensional velocity distributions in the solar wind, with derived moments and with other characteristic helium plasma parameters. In particular, for various parameters the heliocentric radial dependence and the variation with the solar wind flow speed was investigated. Special attention was paid to the influence of Coulomb collisions on limiting ion differential speed and temperature ratio. Many characteristics previously found at 1 AU have been confirmed and observed similarly within the radial interval from the Helios perihelion (~ 0.3 AU) to the earth's orbit. A clear tendency could be established for the ion differential speed to increase with decreasing solar distance and to approach the local Alfvén speed with increasing solar wind velocity. The observed close correlation between Δv_{ap} and v_A and the coincidence of Alfvénic type wave activity with pronounced differential speeds strongly suggest that wave forces are the primary cause of preferential ion acceleration.

The influence of the ubiquitous Coulomb friction on ion energy and momentum exchange has been investigated. Typical collision time scales have been shown to vary within nearly three orders of magnitude for various plasma conditions. Evidence has been found that the collisional coupling is weakest in very fast streams where the largest Δv_{ap} and T_α/T_p values are encountered. On the other hand, in cold, dense, and slow plasma (as observed most purely in connection with magnetic sector boundaries; refer to sections 2 and 3 and to the companion paper by Marsch *et al.* [this issue]), Coulomb collisions were shown to play a role in equalizing ion temperatures and limiting differential ion speeds. It has been suggested that in stream interaction regions and high speed trailing edges macroscopic stream mixing may have some influence on T_α/T_p .

Average temperature gradients for helium ions have been established, yielding a power law dependence on heliocentric radial distance, which in slow plasma is weaker than expected for adiabatic cooling. However, in fast streams the gradients are steeper and $T_{\perp\alpha}$ is compatible with nearly adiabatic behavior within the experimental errors. This is in contrast to the proton observations (compare Marsch *et al.* [this issue]). Temperature anisotropies $T_{\parallel\alpha}/T_{\perp\alpha}$ have been shown to increase slightly from average values of about 1 at 0.3 AU to 1.3 at 1 AU, even though large fluctuations occur.

A variety of differently shaped distributions have been found with experimental confidence. Fairly isotropic distributions were observed in connection with sector boundaries of the IMF. In slow wind well resolved double humped helium ion distributions have sometimes been measured. Their shape was persistent over hours and simultaneously the proton distributions also exhibited a second hump. This phenomenon of 'double ion streams' (see also Feldman *et al.* [1974b] and Asbridge *et al.* [1974]) still represents an unsolved puzzle with regard to its origin and the limitation of the ion differential speed, which is observed to be nearly equal to v_A .

High-speed He^{2+} distributions are often more than ten times hotter than distributions in slow wind and unexpectedly high temperatures of a few $\times 10^6$ K have typically been observed near 0.3 AU. Under these conditions a tendency for the core part of the He^{2+} distribution to be characterized by $T_{\parallel\alpha}/T_{\perp\alpha} > 1$ has been observed. Such an anisotropy is in distinct contrast to the proton core anisotropy, which is considerably less than one. This observation represents a challenge for any detailed theory of ion heating by wave interaction.

Although much progress has been made in describing the helium component of the solar wind plasma, many basic questions remain unanswered. Clearly, the detailed Helios observations have laid further solid experimental grounds but also have given rise to new questions, for example, in connection with the extreme values of T_α/T_p and Δv_{ap} observed in the perihelion. The observed correlations of differences in ion parameters with Alfvénic type wave activity suggest that in the future a more detailed empirical and theoretical investigation of ion-wave interactions may help explain helium ion heating and acceleration in the solar wind.

Acknowledgments. Helpful discussions of one of the authors (E. Marsch) with C. T. Dum, W. G. Pilipp, and R. W. Boswell are gratefully acknowledged. The authors thank M. F. Thomson for a careful reading of the manuscript resulting in valuable comments. The Helios project is jointly conducted and supported by the German Bundesministerium für Forschung und Technologie (BMFT) and the National Aeronautics and Space Administration (NASA) of the USA. The Helios plasma experiment and its data evaluation and scientific interpretation are supported by the BMFT under grants no. WRS 10/7 and WRS 0108.

The Editor thanks K. Ogilvie and M. Neugebauer for their assistance in evaluating this paper.

REFERENCES

- Asbridge, J. R., S. J. Bame, and W. C. Feldman, Abundance differences in solar wind double streams, *Solar Phys.*, **37**, 451, 1974.
- Asbridge, J. R., S. J. Bame, W. C. Feldman, and M. D. Montgomery, Helium and hydrogen velocity differences in the solar wind, *J. Geophys. Res.*, **81**, 2719, 1976.

- Barnes, A., and R. J. Hung, On the kinetic temperature of He^{2+} in the solar wind, *Cosmic Electrodyn.*, **3**, 416, 1973.
- Behannon, K. W., Observations of the interplanetary magnetic field between 0.41 and 1 AU by the Mariner 10 spacecraft, *GSFC X Document 692-76-2*, Goddard Space Flight Center, Greenbelt, Md., 1976.
- Belcher, J. W., and L. Davis, Jr., Large-amplitude Alfvén waves in the interplanetary medium, *J. Geophys. Res.*, **76**, 3534, 1971.
- Bosqued, J. M., C. Duston, A. A. Zertalov, and D. L. Vaisberg, Study of alpha component dynamics in the solar wind using the Prognostic satellite, *Solar Phys.*, **51**, 231, 1976.
- Boyd, T. J. M., and J. J. Sanderson, *Plasma Dynamics*, Barnes and Noble, New York, 1969.
- Burlaga, L. F., Interplanetary stream interfaces, *J. Geophys. Res.*, **79**, 3717, 1974.
- Burlaga, L. F., and K. W. Ogilvie, Solar wind temperature and speed, *J. Geophys. Res.*, **78**, 2028, 1973.
- Denskat, K. U., F. M. Neubauer, and R. Schwenn, Properties of Alfvénic fluctuations near the sun: Helios 1 and Helios 2, in *Solar Wind 4*, edited by H. Rosenbauer, Springer-Verlag, New York, in press., 1981.
- Dusenbery, P. B., and J. V. Hollweg, Ion cyclotron heating and acceleration of solar wind minor ions, *J. Geophys. Res.*, **86**, 153, 1981.
- Feldman, W. D., D. R. Asbridge, S. J. Bame, and M. D. Montgomery, On the origin of solar wind proton thermal anisotropy, *J. Geophys. Res.*, **78**, 6451, 1973.
- Feldman, W. C., J. R. Asbridge, and S. J. Bame, The solar wind He^{2+} to H^+ temperature ratio, *J. Geophys. Res.*, **79**, 2319, 1974a.
- Feldman, W. C., J. R. Asbridge, S. J. Bame, and M. D. Montgomery, Interpenetrating solar wind streams, *Rev. Geophys. Space Phys.*, **4**, 715, 1974b.
- Feynman, J., On solar wind helium and heavy ion temperatures, *Solar Phys.*, **43**, 249, 1975.
- Formisano, V., F. Palmiotto, and G. Moreno, α -Particle observations in the solar wind, *Solar Phys.*, **15**, 479, 1970.
- Geiss, J., P. Hirt, and H. Leutwyler, On acceleration and motions of ions in corona and solar wind, *Solar Phys.*, **12**, 458, 1970.
- Gosling, J. T., J. R. Asbridge, S. J. Bame, and W. C. Feldman, Solar wind stream interface, *J. Geophys. Res.*, **83**, 1401, 1978.
- Grünwaldt, H., and H. Rosenbauer, Study of helium and hydrogen velocity differences as derived from HEOS-2 S-210 solar wind measurements, paper presented at the Second European Solar Meeting, Centre National de la Recherche Scientifique, Toulouse, France, 1978.
- Hirshberg, J., J. R. Asbridge, and D. E. Robbins, The helium component of solar wind velocity streams, *J. Geophys. Res.*, **79**, 934, 1974.
- Hollweg, J. V., Alfvénic acceleration of solar wind helium and related phenomena, 1, Theory, *J. Geophys. Res.*, **79**, 1357, 1974.
- Hollweg, J. V., Helium and heavy ions, in *Solar Wind 4*, edited by H. Rosenbauer, Springer-Verlag, New York, in press., 1981.
- Hollweg, J. V., and J. M. Turner, Acceleration of solar wind He^{2+} , 3, Effects of resonant and nonresonant interactions with transverse waves, *J. Geophys. Res.*, **83**, 97, 1978.
- Hundhausen, A. J., *Coronal Expansion and Solar Wind*, Springer-Verlag, New York, 1972.
- Marsch, E., K.-H. Mühlhäuser, W. Pilipp, R. Schwenn, and H. Rosenbauer, Initial results on solar wind alpha particle distributions as measured by Helios between 0.3 and 1 AU, in *Solar Wind 4*, edited by H. Rosenbauer, Springer-Verlag, New York, in press., 1981a.
- Marsch, E., K.-H. Mühlhäuser, H. Rosenbauer, R. Schwenn, and K. U. Denskat, Pronounced proton core temperature anisotropy, ion differential speed, and simultaneous Alfvén wave activity in slow solar wind at 0.3 AU, *J. Geophys. Res.*, **86**, 9199, 1981b.
- Marsch, E., K.-H. Mühlhäuser, R. Schwenn, H. Rosenbauer, W. Pilipp, and F. M. Neubauer, Solar wind protons: Three-dimensional velocity distributions and derived plasma parameters measured between 0.3 and 1 AU, *J. Geophys. Res.*, this issue.
- McKenzie, J. F., and E. Marsch, Resonant wave acceleration of minor ions in the solar wind, *Astrophys. Space Sci.*, in press, 1981.
- McKenzie, J. F., W. H. Ip, and W. I. Axford, Anomalous acceleration of minor ions in the solar wind, *Nature*, **274**, 350, 1978.
- McKenzie, J. F., W. H. Ip, and W. I. Axford, The acceleration of minor ions in the solar wind, *Astrophys. Space Sci.*, in press, 1981.
- Morfill, G., M. Scholer, A. K. Richter, Average properties of cosmic ray diffusion in solar wind streams, *J. Geophys. Res.*, **84**, 1505, 1979.
- Musmann, G., F. M. Neubauer, A. Maier, and E. Lammers, Das Förstersonden-Magnetfeldexperiment (E2), *Raumfahrtforschung*, **19**, 232, 1975.
- Neubauer, F. M., G. Musmann, and G. Dehmel, Fast magnetic fluctuations in the solar wind: Helios 1, *J. Geophys. Res.*, **82**, 3201, 1977.
- Neugebauer, M., The role of coulomb collisions in limiting differential flow and temperature differences in the solar wind, *J. Geophys. Res.*, **81**, 78, 1976.
- Neugebauer, M., Observations of solar wind helium, *Fundam. Cosmic Phys.*, **7**, 131, 1981.
- Neugebauer, M., and W. C. Feldman, Relation between superheating and superacceleration of Helium in the solar wind, *Solar Phys.*, **63**, 201, 1979.
- Neugebauer, M., and C. W. Snyder, Mariner 2 observations of the solar wind, 1, Average properties, *J. Geophys. Res.*, **71**, 4469, 1966.
- Ogilvie, K. W., Differences between the bulk speeds of hydrogen and helium in the solar wind, *J. Geophys. Res.*, **80**, 1335, 1975.
- Robbins, D. E., A. J. Hundhausen, and S. J. Bame, Helium in the solar wind, *J. Geophys. Res.*, **75**, 1178, 1970.
- Rosenbauer, H., R. Schwenn, E. Marsch, B. Meyer, H. Miggenrieder, M. D. Montgomery, K.-H. Mühlhäuser, W. Pilipp, W. Voges, and S. M. Zink, A survey on initial results of the helios plasma experiment, *J. Geophys.*, **42**, 561, 1977.
- Ryan, J. M., and W. I. Axford, The behavior of minor ion species in the solar wind, *J. Geophys. Res.*, **41**, 221, 1975.
- Schwenn, R., H. Rosenbauer, and H. Miggenrieder, Das Plasmaexperiment auf Helios (E1), *Raumfahrtforschung*, **19**, 226, 1975.
- Schwenn, R., M. D. Montgomery, H. Rosenbauer, H. Miggenrieder, K.-H. Mühlhäuser, S. Bame, W. C. Feldman, and R. T. Hansen, Direct observation of the latitudinal extent of a high speed stream in the solar wind, *J. Geophys. Res.*, **83**, 1011, 1978.
- Schwenn, R., H. Rosenbauer, and K.-H. Mühlhäuser, Singly ionized helium in the driver gas of an interplanetary shock wave, *Geophys. Res. Lett.*, **7**, 201, 1980.
- Schwenn, R., K.-H. Mühlhäuser, E. Marsch, and H. Rosenbauer, Two states of the solar wind at the time of solar activity minimum, 2, Radial gradients of plasma parameters in fast and slow streams, in *Solar Wind 4*, Springer-Verlag, New York, in press., 1981.
- Spitzer, L., Jr., *Physics of Fully Ionized Gases*, 2nd ed., Interscience, New York, 1962.

(Received April 21, 1981;
revised August 3, 1981;
accepted August 24, 1981.)